Development of Performance System With Musical Dynamics Expression on Humanoid Saxophonist Robot

Jia-Yeu Lin, Mao Kawai, Yuya Nishio, Sarah Cosentino, and Atsuo Takanishi

***Abstract*—Talented musicians can deliver a powerful emotional experience to the audience by skillfully modifying several musical parameters, such as dynamics, articulation, and tempo. Musical robots are expected to control those musical parameters in the same way to give the audience an experience comparable to listening to a professional human musician. But practical control of those parameters depends on the type of musical instrument being played. In this study, we describe our newly developed music dynamics control system for the Waseda Anthropomorphic Saxophonist robot. We first built a physical model for the saxophone reed motion and verified the dynamics-related parameters of the overall robot-saxophone system. We found that the magnitude of air flow is related to the sound pressure level, as expected, but also that the lower lip is critical to the sound stability. Accordingly, we then implemented a music dynamics control system for the robot and succeeded in enabling the robot to perform a music piece with different sound pressure levels.**

***Index Terms*—Entertainment robotics, human-centered robotics, humanoid robots.**

I. Introduction

MUSIC is a social activity that can powerfully influence large groups of people. A skillful musician can elicit powerful emotions in the audience by careful modulation of several different musical parameters, such as dynamics, tempo, articulation and pitch [1]. In the emerging field of entertainment robotics, musical robots are attracting attention for their multi-user interactive experience potential [2]. With their musical performance abilities, these robots are expected to entertain and interact with a large crowd.

Manuscript received September 10, 2018; accepted January 13, 2019. Date of publication February 4, 2019; date of current version February 19, 2019. This letter was recommended for publication by Associate Editor H. Rodrigue and Editor Y. Choi upon evaluation of the reviewers' comments. This work was supported by the JSPS Grant-in-Aid for Young Scientists (Wakate B) 17K18178 and ST Microelectronics. *(Corresponding author: Jia-Yeu Lin.)*

J.-Y. Lin, M. Kawai, and Y. Nishio are with the Department of Integrative Bioscience and Biomedical Engineering, Waseda University, Tokyo 169-8050, Japan (e-mail: erin@fuji.waseda.jp; maochan6@akane.waseda.jp; yyns@akane.waseda.jp).

S. Cosentino is with the Department of Modern Mechanical Engineering, Waseda University, Tokyo 169-8050, Japan (e-mail: sarah.cosentino@aoni.waseda.jp).

A. Takanishi is with the Department of Modern Mechanical Engineering and the Human Robotics Institute, Waseda University, Tokyo 169-8050, Japan (e-mail: takanisi@waseda.jp).

Digital Object Identifier 10.1109/LRA.2019.2897372

In the past few years, several robots have been developed to play different kinds of instruments, primarily strings and percussion instruments, where movement precision is of utmost importance. The Toyota humanoid violin robot [3], the Waseda University electronic organ player robot WABOT-2 [4], and the Georgia Tech marimba player robot, Shimon [5], are notable examples. By combining highly accurate visual sensing systems, fast body movement, and real-time feedback, they can perform at a very high level. However, there have been very limited studies on other types of instruments, in particular the woodwinds, due to the difficulty of modeling their non-linear instrument behavior based on air flow dynamics.

A wind instrument consists of a sound generator coupled with a resonator. The sound is amplified in the resonator by a column of air set into vibration when the player blows into the mouthpiece, a sound generator at one end of the apparatus [6]. Wind instruments are highly nonlinear since they rely on fluid dynamics laws for sound production, and playing techniques differ greatly depending on both the instrument and the mouthpiece type. Moreover, sound characteristics are also affected by characteristics of the produced air flow and the configuration of the oral cavity against the instrument. The saxophone, one of the most versatile wind instruments, is commonly used in many musical genres, including classical, jazz, and pop. Saxophone players can play expressively by carefully controlling their perioral muscles and lung movements, shaping the emitted air flow characteristics, and modulating the sound pressure levels (SPL) to obtain the desired music dynamics. Dynamics is in fact closely related to emotional expression in music [7]. The Waseda Anthropomorphic Saxophonist robot (WAS), developed by Waseda University since 2007, can play a typical alto saxophone with mechanisms similar to human players. However, WAS has been unable to change the SPL during performance, reducing greatly the diversity and expressivity of its performance. To solve this problem, in this work we have developed a sound pressure control system to enable the WAS to modulate music dynamics while playing, for a more diverse and expressive performance.

The first step to implement a system mimicking the human mechanisms necessary for modulating sound pressure, thus music dynamics, is to build a physical model of sound production with a saxophone and investigate the parameters that are critical for musical dynamics. There is already a substantial body of

literature on the physics of sound production in reed instruments, both in static and dynamic condition. Dalmont [8] described a method to measure reed characteristics, including its viscoelasticity and stiffness, in a quasi-static condition. Other researchers focused on the reed behavior under direct acoustic excitation. For example, Gazangel [9] used a displacement sensor to measure the reed vibrational response during sound emission, computing and comparing parameters such as the threshold pressure and the spectral centroid. The same team also demonstrated how the reed is a critical component in sound production with a saxophone [10]. By measuring the correlation between perceptual and acoustical data of sound produced using 20 different reeds, they provided scientific data on how reed characteristics affect the sound produced. But these works did not consider the human player, and thus did not model the direct relationship between the player's muscles, organ configurations, produced airflow, and the sound produced by the instrument. The player's physical and physiological configuration is difficult to measure without invasive methods, which inherently alter the configuration itself. This makes modeling and comprehending the overall dynamics extremely difficult.

In this letter, we describe our newly developed music dynamics control system for the WAS robot. To investigate the mechanism of musical dynamics modulation with a saxophone, we built a model of the extended interface between the instrument and the player, with a two-step analysis and validation approach. The first step was to build an original model of a saxophone mouthpiece and reed based on existing models of the reed of a clarinet, a woodwind instrument that is structurally similar to saxophone. We simulated the reed motion to derive the relationship between the robot lip displacement ΔL and pressure difference ΔP between the mouthpiece $(\mathrm{P_{mp}})$ and the oral cavity $(\mathrm{P_m})$. The second step used the WAS robot to perform music repeatedly under the same, quantifiable performing conditions, to validate the accuracy and limitations of the model. Based on the results, we implemented a suitable musical dynamics control system for the WAS.

This letter is organized as follows: Section II explains the robot platform and the concept of musical dynamics. Section III describes the physical model of the saxophone and the experimental protocol used to verify this model. Simulation and experimental results are then compared and discussed in section IV, which also presents the musical dynamics control system implemented using the model and those results. Finally, conclusions and future work on the system are presented in section V.

II. Materials

A. The Anthropomorphic Saxophonist Robot WAS-5

WAS has been under development since 2007 and is currently on its 5th version, as reflected in its name, WAS-5. With 31 degrees of freedom (DoFs), shown in Fig. 1, and mechanisms reproducing the human organs involved in air flow control, the robot is able to play a standard alto saxophone.

In particular, the robot is able to produce and convey the air flow finely into the mouthpiece with an air pump and a proportional valve system mimicking the human airways. In addition,

Body Parts	DoF
Lips	2
Oral Cavity	1
Tongue	1
Lung	2
Finger	19
Waist	1
Gaze	2
Eyebrow	1
Eyelid	2
Total	31

Fig. 1. WAS-5 (Waseda Anthropomorphic Saxophonist Robot Ver.5).

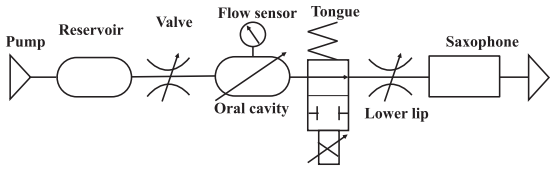

Fig. 2. Pneumatic circuit of WAS-5.

the robot can control the air flow through its oral cavity into the reed with its tongue and artificial lips. The oral cavity and lips are made of Septon, a styrene thermoplastic elastomer developed by Kuraray whose elastic characteristics can be customized as needed by changing the ratio of its reactants. In previous works, the elastic characteristics of human oral cavity and lips were measured while playing a saxophone, and the Septon used for the robot was customized to obtain similar characteristics [11]. Fig. 2 shows the overall pneumatic circuit of WAS-5.

B. Music Dynamics Control

Music dynamics describes the relative loudness levels in a piece of music. Loudness is a subjective psychoacoustic sensation, difficult to clearly define and measure since it is dependent on many parameters, such as sound intensity, frequency, time of exposure to the sound, etc. Among these parameters, sound intensity is a dominating parameter and has been demonstrated to be proportional to the loudness that typical listeners perceived [12]. Sound intensity is proportional to the squared SPL, which can be measured using a sound pressure meter. For this reason, in this work we use SPL as quantifiable signal level related to loudness.

Music dynamics is represented in music with 8 dynamics notation markings, from fortississimo to pianississimo (Table I). The corresponding actual SPL are dependent on a variety of factors: the environment, the performer's interpretation, the instrument itself. In a previous work [13], we measured that the range of sound pressure emitted by an alto saxophone among different pitches ranges from 99.4 – 112.8 [dB]. The measurement was conducted in a soundproof room by using the sound level meter NL-32 placed right above the center of the saxophone's bell, and the noise floor measurement was 67.5 [dB]. We used the same method for all the other measurements described in this letter.

TABLE I
MUSICAL NOTATION OF DYNAMICS

	Notation	MIDI velocity	Loudness
Dynamics	fortississimo	109-127	High
	fortissimo	93-108	
	forte	76-92	
	mezzo-forte	61-75	
	mezzo-piano	46-60	
	piano	31-45	
	pianissimo	11-30	
	pianississimo	0-10	Low

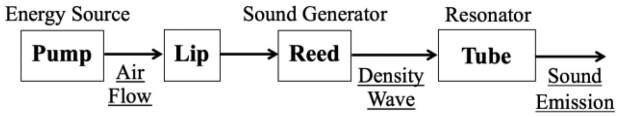

Fig. 3. Sound production of WAS-5.

To play a melody, the control system of the robot reads and transforms in appropriate mechanical commands a MIDI input signal, which includes information such as pitch, tempo and velocity. MIDI velocity represents the musical dynamics, but unfortunately there is no standard conversion of velocity to dynamics [14]. In our work we used a linear conversion curve and translated the 8 different dynamics markings into 8 levels of velocity in the range of 0∼127 (Table I).

III. METHODS

A. System Modeling

The saxophone is a woodwind instrument consisting in a linear resonator and a nonlinear sound generator [15], [16]. The acoustic generator is a reed, which is tightly pressed by the lower lip of a player and generates a pneumatic acoustic density wave when set in vibration by the air jet propelled from the player's mouth. This density wave is then amplified inside the pipe resonator, building up different standing waves according to the player's fingering, and generating different notes. In a previous study [17], it has been found that the reed motion RMS is proportional to the SPL to an extent, until the mouthpiece restriction is reached.

We used the high repeatability of the human-like mechanisms of WAS-5 to investigate and reproduce the human mechanisms involved in dynamics control. First, we built a physical model of the whole system containing the robot configuration and reed motion components to find by simulation all the parameters affecting the sound dynamics. After that, we verified the model and its simulated parameters with the WAS robot. Fig. 3 shows the system diagram of sound production with WAS-5.

The reed can be modeled as an oscillator and the reed motion z(t) as a harmonic oscillation with inertia M, damping C, and spring coefficient K [18]. To describe the deformation of the system composed by the reed and the lower lip during sound emission, we modified the model with two springs connected in series, one representing the reed with coefficient K_R and the other representing the lower lip with coefficient K_L. K_L was

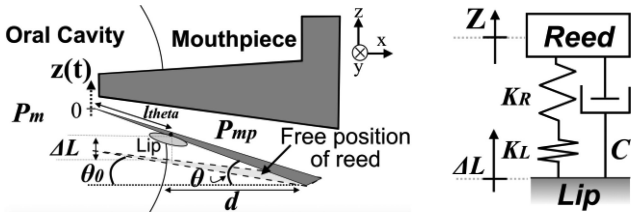

Fig. 4. Schematic view of the mouthpiece-reed-lip system.

TABLE II
DEFINITION AND MEASURED VALUE OF THE PARAMETERS

E: Elastic modulus of reed $(2.7 \cdot 10^9[\text{Pa}])$	l: Length of the reed $(2.1 \cdot 10^{-2}[m])$
I: Second moments of area $(2.9 \cdot 10^{-13}[m^4])$	l_{theta}: Length between the reed tip and the lip
θ_0: Original vertical angel of the reed (8°)	d: Lip position on the reed $(7.7 \cdot 10^{-4}[m])$
W: Reed width $(1.6 \cdot 10^{-3}\ [m])$	M: Reed mass $(1.19[Pa \cdot s^2/m])$
C: Damping of the reed $(0.05[Pa \cdot s/m])$	K_L: Spring coefficient of lip $(2.4 \cdot 10^7[Pa/m])$

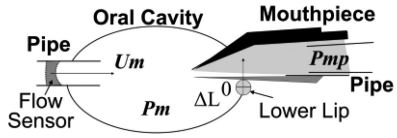

Fig. 5. Experiment setup.

then obtained from a tensile test measuring both the tensile stress and the tensile strain of the soft material used in the robot lip, and computing the material young's modulus. We then modeled the reed as a cantilever beam, with a horizontal angle θ_0 in rest position, when not pressed by the lower lip. To generate sound, the player blows air into the mouthpiece, producing a pressure difference between the mouthpiece (P_{mp}) and the oral cavity (P_m), which can be viewed as an external force on the oscillator system. The air pressure is a uniformly distributed load applied on the reed area. The stiffness K_R for unit area is given in equation (1):

$$K_R = \frac{8EI}{{l_{theta}}^4 \cdot W} = \frac{8EI}{W \cdot (l - d/cos(arctan(\frac{\Delta L}{d} + tan\,(\theta_0)))\ )^4} \quad (1)$$

as a function of lower lip displacement ΔL. The reed motion $z(t)$ is described in equation (2):

$$M\ddot{z}(t) + C\dot{z}(t) + \frac{K_R \cdot K_L}{K_R + K_L} \cdot z\,(t) = P_m - P_{mp} \quad (2)$$

A schematic view of the model is shown in Fig. 4 and all the parameters used in the equations are defined in Table II. Using the WAS robot, we then found out the relationship between generated airflow (U_m) measured from the back of the oral cavity (opposite side of the interface to the mouthpiece, Fig. 5) and air pressure difference ΔP between the oral cavity (P_m) and the mouthpiece (P_{mp}). The mouthpiece with reed at rest is set

TABLE III
COEFFICIENTS OF FLOW-PRESSURE FUNCTION AND DETERMINATION

ΔL[mm]	a(ΔL)[$\frac{min \cdot Pa}{L}$]	b(ΔL)[Pa]	R^2
0	8.66	-6.57	0.849
0.5	9.03	-13.3	0.790
1	15.1	-82.3	0.950
1.5	24.4	-143	0.981
2	44.1	-282	0.997
2.5	71.0	-515	0.993

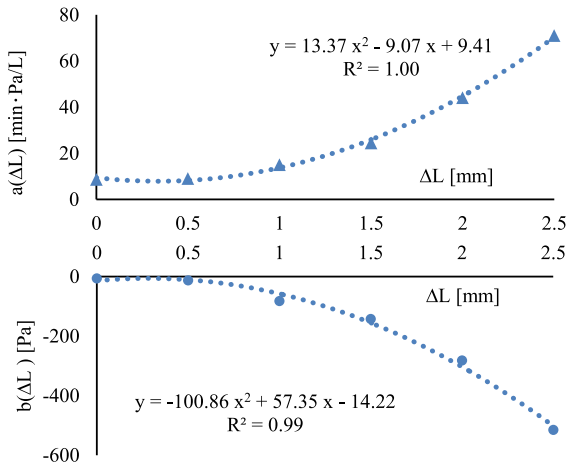

Fig. 6. Analysis of the slope and intercept in flow-pressure function.

on the oral cavity of the robot, with the lower lip slightly attached but not pressing the reed ($\Delta L = 0$). A pressure sensor and a flow sensor were used to measure the pressure and airflow rate inside the robot oral cavity. Another pressure sensor was connected to the rear end of the mouthpiece. We measured the behavior of the system while increasing U_m with a proportional valve in steps of 1.4L/min and lower lip position ΔL increasing by moving closer to the mouthpiece in steps of 0.5mm. The values of ΔL and U_m of all possible combinations for sound production (flow in the range of 14.3 – 26.3L/min and the lower lip at the range of 0 – 2.5mm) were measured. The result is that the relationship between ΔP and U_m is linear no matter how the lip displacement is changed. Furthermore, when conducting regression analysis between ΔP and U_m and changing lip displacement, the slope and y-intercept were found to be functions of ΔL. The relation between ΔP and U_m at different ΔL in the robot could be written as in equation 3.

$$\Delta P = P_m - P_{mp} = a(\Delta L) \cdot U_m + b(\Delta L) \tag{3}$$

The trend line and the coefficient of determination (R^2) of each ΔL is presented in Table III. It can be observed that as ΔL increases, the slope of trend line increases and the intercept decreases. Both parameters can be computed by a quadratic approximation of ΔL (Fig. 6).

B. System Simulation

From the physical model obtained in section A, we derived the relationship between the robot generated airflow U_m, lip displacement ΔL and pressure difference ΔP. Setting the measured ΔP as the external force for unit area in the mass-spring-damper oscillator model, the root mean square (RMS) of the reed oscillating motion can be calculated by substituting the measured parameters into equation 2 (as the procedure shown in Fig. 7). We conducted the simulation of the reed movement by using Matlab/Simulink.

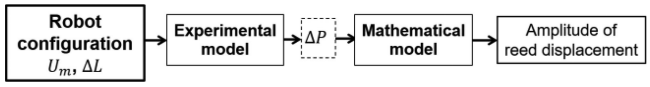

Fig. 7. Block diagram of the simulation.

TABLE IV
PARAMETERS USED IN THE EXPERIMENT

Parameter	Range	Step
Pump rotation speed	150 – 330 [rpm]	1 [L/min] increase
Lower Lip	0 – 0.8[mm]	0.1 [mm] increase
Note	C4, D4, E4, F4, G4	

C. Empirical Experiment

We carried out a series of final experiments to verify the accuracy of the proposed model and to analyze how the actual configuration of the robot affects the SPL.

There are three controllable parameters in the robot: lower lip, pump rotational speed, and fingering. The position of the lower lip can be adjusted by a PID motor position controller. The pump rotational speed can be manipulated by a voltage change with the speed linearly proportional to the produced airflow rate. The note is changed by controlling the fingers pressing on the tone holes. In order to verify the relation between the robot configuration and the sound, all possible combinations for sound production (Table IV) need to be verified. We measured the behavior of the system with the reed vibrating, recording pressure and airflow data at a sample rate of 100Hz, and sound data at a standard sample rate of 44100Hz. The experiment was conducted according to this protocol:

1) **Configuration setting:** the robot fingering, the lower lip position and the pump rotation speed were set.
2) **Data measurement:** Sound was emitted for 4s, and the SPL, pressure, and airflow data were measured for 2s after a latency of 2s to allow sound stabilization and recording of stable data.
3) **Reconfiguration parameters:** One of the parameters was changed and the whole process repeated till all the possible parameters configurations were covered.

IV. RESULTS

A. Simulation Results

The simulation described in section III-B using the physical model yielded the following two relationships.

1) Correlations between airflow rate and reed oscillating motion peak amplitude: by varying the air flow in a range common for saxophone playing, from 18 [L/min]

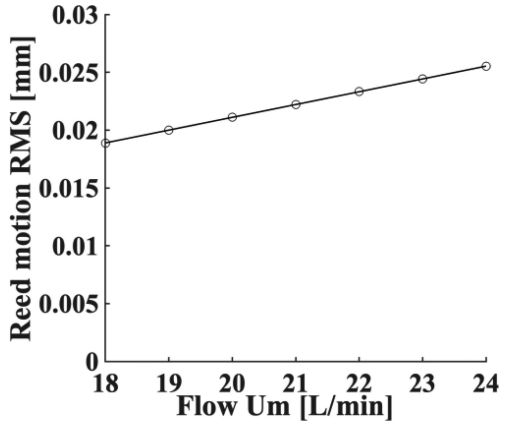

Fig. 8. Simulation result of reed motion RMS and flow ($\Delta L = 0.1$ [mm]).

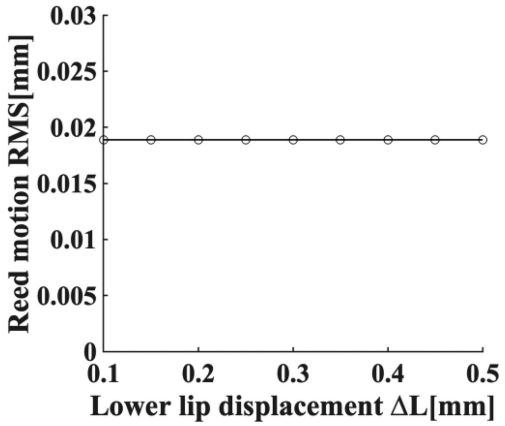

Fig. 9. Simulation result of reed motion RMS and lip displacement ($U_m = 18$ [L/min]).

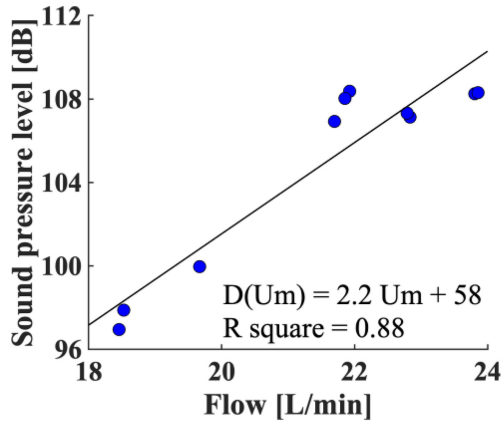

Fig. 10. Relationship between SPL and air flow (Pitch: C4, Lower: 0.7 [mm]).

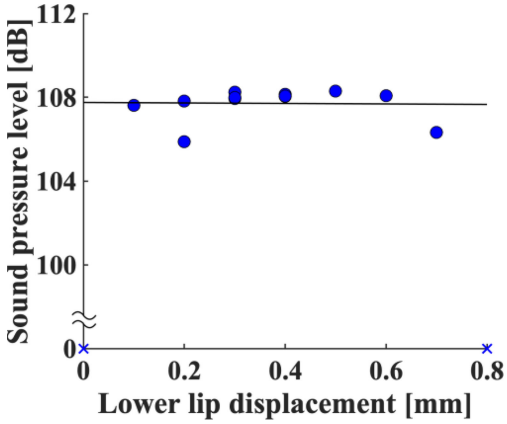

Fig. 11. Relationship between SPL and lower lip displacement (Pitch: C4, Pump: 240 [rpm]).

to 24 [L/min] in the model, the reed motion RMS varies accordingly (Fig. 8).

2) Correlation between lip displacement and reed motion RMS. In the simulation, the stiffness K_R in the model changes depending on different lip displacement setting from 0 [mm] to 0.5 [mm], changing the quadratic mean of reed motion. However, compared to the changes produced by the variation of the airflow, these changes are negligible and can be disregarded (Fig. 9).

As demonstrated previously, reed motion of the reed oscillating motion and SPL are positively correlated.

B. Experimental Results

The results of the empirical experiment revealed the following two relationships:

1) Proportionality between flow U_m and D_{out}. We measured the SPL while changing the flow by setting different pump rotation speeds and maintaining the other parameters fixed. Results show that it is possible to approximate the SPL as a linear relationship to flow (Fig. 10).
2) Correlation between lower-lip displacement ΔL and D_{out}. The SPL changes slightly as lip displacement varies while maintaining the same pump rotation speed on the same note. However, it is negligible and can be ignored compared to the ones depending on the airflow (Fig. 11).

We also compared the experimental results with the simulation results, to find compatible trends and verify the validity range of our simulated mathematical reed motion model. The measurement results show the same trend as in the simulation, which indicates that in order to produce different SPL, we can adjust the input airflow regardless of the lip setting. In addition, Fig. 11 also shows that when ΔL is very small or very large, there is no sound production (SPL = 0, noted by a cross mark). This may be because there is a certain range of lip pressure needed in order to make the reed vibrate [19]. The reed will not be able to vibrate if there is insufficient lip pressure to provide a pivot, while excessive pressure will press the reed close against the mouthpiece. Only when the reed is between these two extremes, will it be able to vibrate and produce sound, according to the simulated mathematical reed motion model.

These results imply two important points. First, in addition to the SPL control, it is important for our system to maintain the oral pressure in a certain range to preserve continual sound production. Second, the oral pressure may have a correlation with the lower lip displacement ΔL. Therefore, we also investigated the relation between oral pressure and lower lip displacement ΔL when there was sound production in the experiment. Fig. 12

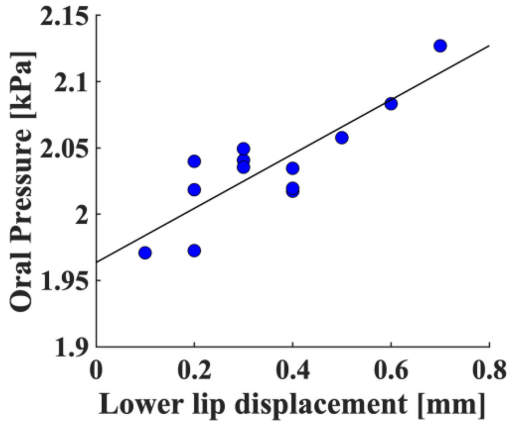

Fig. 12. Relationship between oral pressure and lower lip displacement (Pitch: C4).

shows the results with one configuration. As shown, within the boundary allowing sound production for the saxophone, the oral pressure always increased linearly as the lower lip displacement increased.

C. Results Discussion

The results of the simulation and the empirical verification experiment on the actual robot confirm the accuracy of the model and provide the basis for the music dynamics control system. Moreover, the experimental results also show the importance of lip displacement to ensure continuous sound emission, which results in hard pressure boundaries in the model. These boundaries are critical for sound emission and need to be considered in the control system.

D. Sound Dynamics Control System

Considering both the physical model simulation and the experiment results, we developed a control system with a double scope: control of music dynamics and stabilization of sound emission. This control system works with any MIDI input. From the MIDI velocity data of each note, the corresponding dynamics marking is obtained. The obtained dynamics marking, is labeled with one of 8 different sound levels, corresponding to different SPL, from softest to loudest. Exploiting the linear relationship between flow and SPL obtained in the empirical experiment, we can also divide the airflow into 8 different levels as shown in equation 4:

$$U_n = U_{min} + \frac{(U_{max} - U_{min})}{8} \times (n-1) \qquad n = 1 \sim 8 \tag{4}$$

As the flow increases, the SPL can also be increased. Here, the notation U_{min} represents the smallest flow enabling sound production, and U_{max} represents the largest flow the robot can produce. Therefore, from the sound level determined from the MIDI signal, we can decide the command value of the flow. To meet the system specifications, the airflow in the oral cavity needs to be controlled precisely and rapidly. We added a proportional valve after the pump for rapid and precise airflow control. The valve also enables a proportional control of airflow, permitting the definition of 8 different levels of airflow corresponding to 8 different SPL associated to the 8 musical dynamics markings. Fig. 13 shows the control system block diagram. It is separated functionally into two parts, a part controlling the SPL, and a part stabilizing the oral pressure to ensure continuous sound emission.

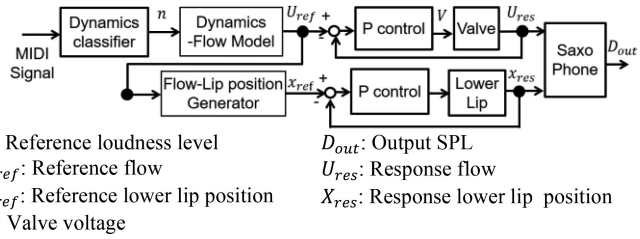

Fig. 13. Dynamics expression control system.

As previously mentioned, the reed can vibrate and emit sound only within a certain range of oral pressure. Therefore, to stabilize the sound and ensure continuous sound emission, we select a suitable lower lip position according to the reference airflow and use proportional control to adjust it. We control the oral pressure with the positioning of the lower lip because, as shown previously, there is linear correlation between oral pressure and lower lip displacement. Moreover, the correlation between lower lip displacement and SPL is negligible and can be disregarded. This is very important because it allows the separation between the pressure stabilization system and musical dynamics control system.

As different SPL require different oral pressure ranges, we defined the lower lip position range boundaries for the nth sound level as x_{n_min} and x_{n_max}, and we set the reference value of lower lip position for each SPL as the mean of the lower and upper boundary, as in equation 5:

$$\mathrm{x}_{n\_ref} = \frac{\mathrm{x}_{n\_max} + \mathrm{x}_{n\_min}}{2} \tag{5}$$

To conclude, from the input MIDI signal, the target SPL for each note can be determined. By using the corresponding input airflow from the valve for volume control and proper lower lip position for sound stability, we can produce 8 different SPL associated to the 8 different musical dynamics markings.

V. Conclusion

In this work, we describe our newly developed music dynamics control system for the Waseda Anthropomorphic Saxophonist robot. First, we modeled the mechanisms of the system to change music dynamics. In particular, we devised and simulated a reed vibration model, critical for producing sound in wind instruments. Simulation of the model dynamics, later confirmed with an empirical experiment with the robot, showed that SPL has a positive correlation with airflow while is independent from lower lip displacement. However, in the experiment with the robot, we found that the lower lip displacement affects the oral pressure, which needs to be stabilized to emit a continuous sound.

As a result, the developed control system uses flow to control the SPL and lower lip displacement to stabilize the sound emission. This control system enables the robot to play music at 8 different SPL, corresponding to the musical dynamics marking.

In the future, evaluation and comparison of the acoustical and perceptual aspects of the system should be conducted. Since the main purpose of this study was to allow more expressive robot performance, we should also conduct a questionnaire-based experiment investigating how the system affects the audience perception of the performance. We will also combine the mechanism used for reproducing human body movements with the different dynamics. By doing so, the robot can give a more human-like impression, possibly increasing the effectiveness of audience interaction.

ACKNOWLEDGMENT

The authors would also like to express their thanks to Tokyo Women's Medical University/Waseda University Joint Institution for Advanced Biomedical Sciences (TWIns) and Humanoid Robotics Institute (HRI) for their assistance to this work.

REFERENCES

[1] R. Bresin and A. Friberg, "Emotion rendering in music: Range and characteristic values of seven musical variables," *Cortex*, vol. 47, no. 9, pp. 1068–1081, Oct. 2011.

[2] A. Kapur, "A history of robotic musical instruments," in *Proc. Int. Comput. Music Conf.*, San Francisco, CA, USA, 2005, pp. 21–28.

[3] D. Sanders and Y. Kusuda, "Toyota's violin-playing robot," *Ind. Robot Int. J.*, vol. 35, no. 6, pp. 504–506, 2008.

[4] I. Kato *et al.*, "The robot musician 'wabot-2' (waseda robot-2)," *Robotics*, vol. 3, no. 2, pp. 143–155, Jun. 1987.

[5] G. Hoffman and G. Weinberg, "Shimon: An interactive improvisational robotic marimba player," in *Proc. Int. Conf. Human Factors Comput. Syst.*, New York, NY, USA, 2010, pp. 3097–3102.

[6] E. Ducasse, "A physical model of a single-reed wind instrument, including actions of the player," *Comput. Music J.*, vol. 27, no. 1, pp. 59–70, 2003.

[7] S. B. Kamenetsky, D. S. Hill, and S. E. Trehub, "Effect of tempo and dynamics on the perception of emotion in music," *Psychol. Music*, vol. 25, no. 2, pp. 149–160, Oct. 1997.

[8] J.-P. Dalmont, J. Gilbert, and S. Ollivier, "Nonlinear characteristics of single-reed instruments: Quasistatic volume flow and reed opening measurements," *J. Acoust. Soc. Amer.*, vol. 114, no. 4, pp. 2253–2262, Oct. 2003.

[9] B. Gazengel, J.-F. Petiot, and M. Oltés, "Objective and subjective characterization of saxophone reeds," in *Proc. Acoust.*, Nantes, France, 2012, pp. 1750–1754.

[10] J.-F. Petiot, P. Kersaudy, G. Scavone, S. McAdams, and B. Gazengel, "Investigation of the relationships between perceived qualities and sound parameters of saxophone reeds," *Acta Acustica United Acustica*, vol. 103, no. 5, pp. 812–829, 2017.

[11] J.-Y. Lin, M. Kawai, K. Matsuki, S. Cosentino, S. Sessa, and A. Takanishi, "Musical articulation system on humanoid saxophonist robot," in *ROMANSY 22–Robot Design, Dynamics and Control*, Berlin, Germany: Springer, 2019, pp. 392–399.

[12] S. S. Stevens, "The measurement of loudness," *J. Acoust. Soc. Amer.*, vol. 27, no. 5, pp. 815–829, 1955.

[13] J.-Y. Lin, "Research on humanoid saxophone playing robot—development of performance system with rich dynamic expression," M.S. thesis, Graduate School Adv. Sci. Eng., Waseda Univ., Tokyo, Japan, 2017.

[14] A. E. Coca, G. O. Tost, and L. Zhao, "Characterizing chaotic melodies in automatic music composition," *Chaos, Interdisciplinary J. Nonlinear Sci.*, vol. 20, no. 3, Sep. 2010, Art. no. 033125.

[15] N. H. Fletcher, "Nonlinear theory of musical wind instruments," *Appl. Acoust.*, vol. 30, no. 2, pp. 85–115, Jan. 1990.

[16] A. Hirschberg, J. Gilbert, R. Msallam, and A. Wijnands, "Shock waves in trombones," *J. Acoust. Soc. Amer.*, vol. 99, no. 3, pp. 1754–1758, 1996.

[17] J. Backus, "Vibrations of the reed and the air column in the clarinet," *J. Acoust. Soc. Amer.*, vol. 33, no. 6, pp. 806–809, Jun. 1961.

[18] A. Muñoz Arancón, B. Gazengel, J.-P. Dalmont, and E. Conan, "Estimation of saxophone reed parameters during playing," *J. Acoust. Soc. Amer.*, vol. 139, no. 5, p. 2754–2765, May 2016.

[19] A. Młyńska, "Reed function in clarinet physical model," in *Proc. New Trends Audio Video/Signal Process. Algorithms, Architectures, Arrangements Appl.*, 2008, pp. 51–54.